Structural, electronic, optical, and mechanical properties of perovskite materials $RbInX_3$ (X = Cl, Br): First principle investigations

Roll: 161318

Session: 2016-2017

Report submitted to the Department of Physics at
Jashore University of Science and Technology
in partial fulfillment of the requirements
for the degree of Bachelor of science
with Honours in Physics

January, 2022

Abstract

We report structural, electronic, optical, and mechanical properties of cubic perovskite $RbInX_3$ (X=Cl, Br) are calculated using the full-potential linearized augmented plane wave method in the density functional theory as implemented in WIEN2k code is successfully predicting. The exchange-correlation potential is evaluated using generalized gradient approximation. The calculations of electronic band structure, the density of states show that both compounds have no bandgap. The density of states also revealed the metallic nature of these compounds. We have derived the bulk modulus for $RbInCl_3$. We have found that the elastic constant C_{11} and C_{12} are in good correlation with the bonding properties. Bulk modulus B was determined based on the computed values of independent elastic constants C_{11} and C_{12}. According to our result, both compounds have a metallic appearance. These perovskite compounds are excellent metallic conductors and photovoltaic application is not possible.

Acknowledgment

Primarily, I would thank god for being able to complete this project with success. Then I would like to thank my honorable supervisor, Dr. Mohammad Abdur Rashid, his valuable guidance has been the success of his suggestion and his instruction has served as the major contributor towards the completion of the project.

I'm also grateful to the writers of several articles (included in the bibliography), from which I've gleaned a wealth of additional data. I would like to thank my group members and my classmates who helped me a lot.

I would never forget to pay thanks to my parents from the core of my heart for their love and prayers that have always been a source of courage and confidence for me and key to success.

I am making this project not only for marks but also to increase my knowledge. Thanks again to all who helped me.

Contents

List of figures

List of Tables

Structural, electronic, optical, and mechanical properties of perovskite materials $RbInX_3$ (X = Cl, Br): First principle investigations

Chapter 1

Introduction

We are presenting a project assignment on the structural, electronic, elastic, and optical properties of perovskite materials $RbInX_3$ (X = Cl, Br) in this project we tried to give all the important things and information about the project. A project $RbInX_3$ (X = Cl, Br) is an activity that helps us to improve our planning and critical thinking ability. The system name is $RbInX_3$ (X= Cl, Br) of perovskite-type, a compound crystallizing in a cubic system. The cubic crystals of $RbInX_3$ (A is a cation with a different valance or is the second most reactive metal, B is a conductive metal that is not an alkali metal and X is a halide) type which crystallize in a perovskite-like structure are acousto-optic materials of interest [1]. We have done systematic calculations for the lead-free perovskite $RbInX_3$ (X = Cl, Br) in this paper. Perovskite materials have emerged as the most promising and efficient low-cost energy materials for various optoelectronic and photonic device applications.

Perovskite materials' unusual physical features, such as high absorption coefficient, long-range ambipolar charge transfer, low exciton-binding energy, high dielectric constant, ferroelectric properties, and so on, have sparked a lot of interest in optoelectronic and photovoltaic applications. Different classes of perovskite materials, such as chalcogenide perovskite (AMO_3) and halide perovskite (ABX_3) that are again classified as alkali halide and organometal halide, were widely studied. The superior ferroelectric and superconducting properties of

oxide-based perovskites were extensively studied for various applications. In the case of metal halide perovskites, mainly Rubidiam Indiam halide perovskites are the most popular ones [2]. Although the most common perovskite compounds contain oxygen, there are a few perovskite compounds that form without oxygen. Chloride perovskites such as $RbInX_3$ (X=Cl, Br) are well known.

Density-functional theory (DFT) is a successful theory to calculate the electronic structure of atoms, molecules, and solids. Its goal is the quantitative understanding of material propertiesfrom the fundamental laws of quantum mechanics. DFT is a method of obtaining an approximate solution to the Schrodinger equation of a many-body system. We like the method such as density functional theory because it has a good ratio between performance and computational cost. This is still one of the major advantages of the method Hartree and Fock took the initial steps toward solving the complicated and analytically inaccessible many-body Schrödinger equation by developing a set of self-consistent, wave-function based equations allowed for iterative calculations of energy and other necessary parameters [3].

The WIEN2k package is a computer program written in Fortran which performs quantum mechanical calculations on periodic solids. It uses the full-potential (linearized) augmented plane-wave and local-orbitals [FP-(L)APW+lo] basis set to solve the Kohn–Sham equations of density functional theory. WIEN2k was originally developed by Peter Blaha and Karlheinz Schwarz from the Institute of Materials Chemistry of the Vienna University of Technology. The first public release of the code was done in 1990 [4]. Then, the next releases were WIEN93, WIEN97, and WIEN2k [5]. WIEN2k uses density functional theory to calculate the electronic structure of a solid. It is based on the most accurate scheme for the calculation of the bond structure-the full potential energy (linear) augmented plane wave ((L) APW) + local orbit (lo) method. Generalized gradient approximation (GGA) can be used in density universal information.

In this chapter, we start by introducing $RbInX_3$ (X= Cl, Br). In the chapter, we have discussed perovskite materials. In chapter 2 we discussed the basic quantum mechanics that the wave function is the first step in the process. This part contains the article about the Schrödingers groundbreaking equation, time-dependent equation, the wave function, the Hartree Fock approach, and the limitations and fallings of the Hartree Fock approach. Chapter 3 contains the theoretical investigations of density functional theory (DFT). We have discussed a new base variable – the electron density, Thomas fermi theory, The Hohenberg – Khon theorems, The

khon sham equations, The exchange-correlation Functionals, Local density Approximation (LDA), Generalized-Gradient Approximation (GGA). In chapter 4 the calculation part of this project is presented. Firstly we will discuss the Crystallographic structure of both perovskite materials like RbInX3 (Cl, Br). The full potential linearized augmented plane wave (FP-LAPW) approach is used throughout the Wien2k code to complete all calculations. The space group 221 Pm-3m was used to determine the atomic location and space group of the $RbInX_3$

(X=Cl, Br) chemical in the unit cell. $RbInX_3$ (X=Cl, Br) is a perovskite-type chemical with cubic crystallization. We were tested on all of the substances that were investigated. We calculate the self-consistent field (SCF), the bandstructure, the density of state (DOS). According to our result, $RbInX_3$ (X=Cl, Br) is a metal and has no bandgap. Therefore, electronic, optical, elastic, and structural properties of $RbInX_3$ (X= Cl, Br) are still undercover; hence the compound needs further investigation. The elastic constants (C_{11}, C_{12}), bulk modulus are also calculated and discussed. Bulk modulus is a very important mechanical property of solid materials. It indicates the ability of a material to resist compression under applied force and also represents the nature of chemical bonding in solids. Also, we discuss the optical properties of studied compounds are explained in terms of real & imaginary dielectric tensor, optical absorption, reflectivity, and refractivity. The paper aims to obtain electronic, structural, elastic, and optical properties of $RbInX_3$ (X= Cl, Br) and to give some theoretical information about the compound for further investigations. Finally, in chapter 5 we discussed the overall summary of this report.

Chapter 2

Basic Quantum Mechanics

2.1 Schrödinger groundbreaking equation

In 1926, Erwin Schrödinger attempted to describe matter waves by using de Broglie's connections to describe hypothetical plane waves, resulting in the most generic form of the famous equation named after him, the time-dependent Schrödinger equation [6].

$$i\hbar \frac{\partial}{\partial t}\Psi(\vec{r}, t) = \hat{H}\Psi(\vec{r}, t) \tag{2.1}$$

Because using a complete relativistic formulation of the formula is often impractical, Schrödinger proposed a non-relativistic approximation, which is now widely used, particularly in quantum chemistry.

Using the Hamiltonian for a single particle

$$\hat{H} = \hat{T} + \hat{V} = -\frac{\hbar^2}{2m}\vec{\nabla}^2 + V(\vec{r}, t) \tag{2.2}$$

Leads to the (non-relativistic) time-dependent single-particle Schrödinger equation

$$i\hbar\frac{\partial}{\partial t}\Psi(\vec{r}, t) = [-\frac{\hbar^2}{2m}\vec{\nabla}^2 + V(\vec{r}, t)]\hat{H}\Psi(\vec{r}, t) \tag{2.3}$$

Only non-relativistic instances will be studied in this thesis from now on.

$$\hat{H} = \sum_{i=1}^{N} -\frac{\hat{p}_i^{\,2}}{2m_i} + V(\vec{r}_1,\vec{r}_2 \ldots., \vec{r}_N, t) = -\frac{\hbar^2}{2}\sum_{i=1}^{N}\frac{1}{m_i} + V(\vec{r}_1, \vec{r}_2 \ldots. \vec{r}_N, t). \quad (2.4)$$

The corresponding Schrödinger equation reads

$$i\hbar\frac{\partial}{\partial t}\Psi(\vec{r}_1, \vec{r}_2 \ldots., \vec{r}_N, t) = [-\frac{\hbar^2}{2}\sum_{i=1}^{N}\frac{1}{m_i}\nabla_i^{\,2} + V(\vec{r}_1, \vec{r}_2 \ldots. \vec{r}_N, t)]\, \Psi(\vec{r}_1, \vec{r}_2 \ldots., \vec{r}_N, t) \quad (2.5)$$

2.2 Time-independent equation

The solutions of the time-independent Schrödinger equation, in which the Hamiltonian has no time dependence (which implies a time-independent potential $V(\vec{r}_1, \vec{r}_2 \ldots\ldots, \vec{r}_N)$ and the solutions, therefore, describe standing waves which are called stationary states or orbitals. The time-independent Schrödinger equation is not only simpler to solve, but understanding its solutions also provides essential insight into how to solve the time-dependent Schrödinger equation.

The separation of variables approach is used to obtain the time-independent equation, in which the spatial and temporal parts of the wave function are separated [7].

$$\Psi(\vec{r}_1, \vec{r}_2 \ldots., \vec{r}_N, t) = \Psi(\vec{r}_1, \vec{r}_2 \ldots., \vec{r}_N)\, \tau(t) = \Psi(\vec{r}_1, \vec{r}_2 \ldots., \vec{r}_N).\, e^{-i\omega t} \quad (2.6)$$

In addition, the L.H.S of the equation reduces to the Hamiltonian's energy eigenvalue multiplied by the wave function, yielding the general eigenvalue equation.

$$E\Psi(\vec{r}_1, \vec{r}_2 \ldots..,\vec{r}_N, t) = \hat{H}\, \Psi(\vec{r}_1, \vec{r}_2 \ldots..,\vec{r}_N, t \quad (2.7)$$

The Schrödinger equation is rewritten using the many-body Hamiltonian once again

$$E\Psi(\vec{r}_1, \vec{r}_2 \ldots., \vec{r}_N) = [-\frac{\hbar^2}{2}\sum_{i=1}^{N}\frac{1}{m_i}\nabla_i^{\,2} + V(\vec{r}_1, \vec{r}_2 \ldots., \vec{r}_N]\, \Psi(\vec{r}_1, \vec{r}_2 \ldots., \vec{r}_N) \quad (2.8)$$

2.3 The wave function

The word "wave function" was used several times in the last section. As a result, and to better comprehend what follows, a closer examination of the wave function is undertaken.

The first and most essential premise is that a particle's state is fully represented by its (time-dependent) wave function, which means that the wave function contains all information about the particle's state.

The discussion will be limited to the time-independent wave function for the sake of simplicity. When it comes to physical quantities, there's always the subject of possible interpretations as well as observations. A basic premise of the Copenhagen interpretation of quantum mechanics is the Born probability interpretation of the wave function, which provides a physical interpretation for the square of the wave function as a probability density.

$$|\Psi(\vec{r}_1, \vec{r}_2 \ldots\ldots, \vec{r}_N)|^2, d\vec{r}_1 d\vec{r}_2 \ldots d\vec{r}_N \quad (2.9)$$

Equation 2.9 describes the probability that particles 1, 2,..., N are located simultaneously in the corresponding volume element $d\,\vec{r}_1, d\,\vec{r}_2, \ldots\ldots, d\vec{r}_N$, [8]. It is also important to think about what occurs if two particles' locations are swapped. Following purely logical reasoning, such an exchange cannot affect the overall probability density, i.e.

$$|\Psi(\vec{r}_1, \vec{r}_2 \ldots\ldots, \vec{r}_i, \vec{r}_j, \ldots, \vec{r}_N)|^2 = |\Psi(\vec{r}_1, \vec{r}_2 \ldots\ldots, \vec{r}_j, \vec{r}_i, \ldots, \vec{r}_N)|^2 \quad (2.10)$$

The wave function's behavior during a particle exchange can only be one of two a result of the exchange. This is the same as bosons (particles with integer or zero spins) things. The first is the asymmetrical wave function, which remains unchanged as

Another alternative is an anti-symmetrical wave function, in which a significant change is caused by the exchange of two particles, which corresponds to fermions [9-10]. Only electrons, which are fermions, are of interest in this book. The Pauli principle asserts that no two electrons can occupy the same state, where state refers to the orbital and spin components of the wave function. (An explanation of the term spin coordinates will be provided later). The anti-symmetry principle can be thought of as Pauli's quantum-mechanical formalization. In the description of spectra, there are several theoretical concepts to consider (e.g.alkaline doublets) [11]. The normalizing of the wave function is another result of the probability interpretation. If equation (9) describes the chance of finding a particle in a volume element, then using the entire range of coordinates as the volume element must yield a probability of one, implying that all particles must be found someplace in space. This is the same as the wave function's normalizing condition

$$\int d\,\vec{r}_1, \int d\,\vec{r}_2, \ldots \ldots \int d\vec{r}_N \, |\Psi(\vec{r}_1, \vec{r}_2 \ldots\ldots, \vec{r}_N|^2 = 1 \quad (2.11)$$

Equation (11) reveals the specifications that a wave function must meet to be physically acceptable. Wave functions must be square-integrable and continuous over the entire spatial range.[12] Calculating the expectation values of operators with a wave function also yields the

expectation value of the appropriate observable for that wave function, which is a very useful trait[13]. For an observable O ($\vec{r}_1, \vec{r}_2$ …..,$\vec{r}_N$) this can generally be written as

$$O = < O > = \int d\,\vec{r}_1, \int d\,\vec{r}_2, \ldots \ldots \int d\vec{r}_N\, \psi*(\vec{r}_1, \vec{r}_2 \ldots\ldots, \vec{r}_N)\hat{O}\Psi(\vec{r}_1, \vec{r}_2 \ldots\ldots, \vec{r}_N) \quad (2.12)$$

2.5 The Hartree-Fock approach

Variational calculus, which is related to the least-action principle of classical mechanics, is a very valuable tool for determining a good strategy for approximating the analytically not accessible solutions to many-body problems. The ground state wave function 0 corresponds to the lowest energy of the systemE_0, and was calculated using variational calculus. It is possible to approach A good resource for learning about the fundamentals of variational calculus is the literature.T. Fliebach [14] has given this information.

As a result, for the time being, only the electronic Schrödinger equation is of importance, so we will focus on that in the following parts $\hat{H} \equiv \hat{H}_{el},\ E \equiv E_{el}$.

$$E_{trial} \geq E_0 \quad (2.14)$$

With

$$E_{trial} = \int d\,\vec{r}_1, \int d\,\vec{r}_2, \ldots \ldots \int d\vec{r}_N\, \Psi^*_{trial}(\vec{r}_1, \vec{r}_2 \ldots\ldots, \vec{r}_N)\hat{H}\,\Psi_{trial}(\vec{r}_1, \vec{r}_2 \ldots\ldots, \vec{r}_N) \quad (2.15)$$

And

$$E_o = \int d\,\vec{r}_1, \int d\,\vec{r}_2, \ldots \ldots \int d\vec{r}_N\, \psi*(\vec{r}_1, \vec{r}_2 \ldots\ldots, \vec{r}_N)\hat{H}\,\Psi(\vec{r}_1, \vec{r}_2 \ldots\ldots, \vec{r}_N) \quad (2.16)$$

The terms listed above are inconvenient to work with most of the time. The bra-ket notation of Dirac is introduced in the following for the sake of succinct notation. The reader is directed to the original publication for a more complete description of this notation [15].

In that notation, equations (2.20) to (2.22) are expressed as

$$\langle \Psi_{\text{trial}} | \hat{\text{H}} | \Psi_{\text{trial}} \rangle = \text{E}_{\text{trial}} \geq \text{E}_0 = \langle \Psi_0 | \hat{\text{H}} | \Psi_0 \rangle \quad (2.17)$$

Proof: The eigenfunctions ψ_i of the Hamiltonian $\hat{H}$ (each corresponding to an energy eigenvalue E_i) form a complete basis set, therefore any normalized trial wave function ψ_{trial} can be expressed as a linear combination of those eigenfunctions

$$\Psi_{\text{trial}} = \sum_i \lambda_i \psi_i \quad (2.18)$$

The eigenfunctions are assumed to be orthogonal and normalized in this case. As a result of the request to normalize the trial wave function, it follows that

$$\langle \Psi_{trial} \, | \Psi_{trial} \rangle = \langle \sum_i \lambda_i \Psi_i \, | \sum_j \lambda_j \Psi_j \rangle = \sum_i \sum_j \lambda_i^* \lambda_j \langle \Psi_i \, | \Psi_j \rangle = |\lambda_j|^2 \quad (2.19)$$

On the other hand, following (2.17) and (2.19)

$$E_{trial} = \langle \Psi_{trial} \, | \widehat{H} | \Psi_{trial} \rangle = \langle \sum_i \lambda_i \Psi_i \, | \widehat{H} | \sum_j \lambda_j \Psi_j \rangle = \sum_j E_j \, |\lambda_j|^2 \quad (2.20)$$

In addition, the ground state energy E_0 is the lowest possible energy per definition, and therefore has the smallest eigenvalue ($E_0 \leq E_i$), it is found that

$$E_{trial} = \sum_j E_j \, |\lambda_j|^2 \geq E_0 \sum_j |\lambda_j|^2 \quad (2.21)$$

what is similar to an equation (2.17)

One of the main concepts of density functional theory is the mathematical framework employed above, i.e. rules that assign numerical values to functions, also known as functional. A function receives a numerical input and produces a numerical output, whereas a functional receives a function and produces a numerical output [16].

Equations (2.13 to 2.21) also contain that a search for the lowest energy value when applied on all allowed N- electron wave functions will always provide the ground-state wave function. Expressed in terms of functional calculus, where $\Psi \rightarrow \mathrm{N}$ addresses all allowed N-electron wave functions, this indicates [17].

$$E_0 = \min_{\Psi \rightarrow \mathrm{N}} E[\Psi] = \min_{\Psi \rightarrow \mathrm{N}} \langle \Psi | \widehat{H} | \Psi \rangle = \min_{\Psi \rightarrow \mathrm{N}} \langle \Psi | \widehat{T} + \widehat{V} + \widehat{U} \, | \Psi \rangle. \quad (2.22)$$

Due to the vast number of alternative wave functions on one hand and computer power and time constraints on the other, this search is essentially unfeasible for N-electron systems. What is possible is the restriction of the search to a smaller subset of the possible wave function, as it is done in the Hartree-Fock approximation.

In the Hartree-Fock approach, the search is restricted to approximations of the N-electron wave function by an antisymmetric product of N (normalized) one-electron wave-functions, the so-called spin-orbitals $\chi_i(\bar{x}_i)$. A wave function of this type is called Slater-determinant and reads [17, 18].

$$\Psi_0 \approx \emptyset_{SD} = (N!)^{-\frac{1}{2}} \begin{bmatrix} \chi_1(\bar{x}_1) & \cdots & \chi_N(\bar{x}_1) \\ \vdots & \ddots & \vdots \\ \chi_1(\bar{x}_N) & \cdots & \chi_N(\bar{x}_N) \end{bmatrix} \tag{2.23}$$

It is important to notice that the spin-orbitals $\chi_i(\bar{x}_i)$ are not only depending on spatial coordinates but also on a spin coordinate which is introduced by a spin function, $\bar{x}_i = \bar{r}_i, s$.

Returning to the variational principle and equation (2.22), the ground state energy approximated by a single Slater determinant becomes

$$E_0 = \min_{\emptyset_{SD} \to N} E[\emptyset_{SD}] = \min_{\emptyset_{SD} \to N} \langle \emptyset_{SD} | \widehat{H} | \emptyset_{SD} \rangle = \min_{\emptyset_{SD} \to N} \langle \emptyset_{SD} | \widehat{T} + \widehat{V} + \widehat{U} | \emptyset_{SD} \rangle \tag{2.24}$$

A general expression for the Hartree-Fock Energy is obtained by usage of the Slater determinant as a trial function

$$E_{HF} = \langle \emptyset_{SD} | \widehat{H} | \emptyset_{SD} \rangle = \langle \emptyset_{SD} | \widehat{T} + \widehat{V} + \widehat{U} | \emptyset_{SD} \rangle \tag{2.25}$$

For the sake of brevity, a detailed derivation of the final expression for the Hartree-Fock energy is omitted. It is a straightforward calculation found for example in the Book by Schwabl [19].

The final expression for the Hartree-Fock energy contains three major parts: [17].

$$E_{HF} = \langle \emptyset_{SD} | \widehat{H} | \emptyset_{SD} \rangle = \sum_i^N \langle i | \hat{\mathrm{h}} | i \rangle + \frac{1}{2} \sum_i^N \sum_j^N [\langle ii|jj\rangle - \langle ij|ji\rangle] \tag{2.26}$$

With

$$\langle i | \hat{\mathrm{h}} | i \rangle = \chi^*{}_i(\bar{x}_i) \left[-\frac{1}{2} \overrightarrow{\nabla_i^2} - \sum_{k=1}^M \frac{Z_k}{r_{ik}} \right] \chi_i(\bar{x}_i)\, d\bar{x}_i \tag{2.27}$$

$$\langle ii|jj\rangle = \iint |\chi_i(\bar{x}_i)|^2 \frac{1}{r_{ij}} \left|\chi_j(\bar{x}_j)\right|^2 d\bar{x}_i\, d\bar{x}_j, \tag{2.28}$$

$$\langle ii|jj\rangle = \iint \chi_i(\bar{x}_i)\, \chi^*{}_j(\bar{x}_j) \frac{1}{r_{ij}} \chi_j(\bar{x}_j)\, \chi^*{}_i(\bar{x}_i)\, d\bar{x}_i\, d\bar{x}_j \tag{2.29}$$

The kinetic energy and nucleus-electron interactions are represented by the first term, with $\hat{h}$ designating the Hamiltonian's single-particle contribution. The electron-electron interactions are represented by the second and third terms. Coulomb and exchange integrals are the two terms used to describe them [17, 18]. Examination of equations (2.26) to (2.29) furthermore reveals that the Hartree-Fock energy can be expressed as a function of the spin orbitals E_{HF} = E[{χ_i}]. Thus, variation of the spin orbitals leads to the minimum energy [17].

The spin orbitals stay orthonormal during minimization, which is a crucial feature to keep in mind. The Hartree-Fock equations are then restricted by using Lagrangian multipliers λ_i in the resultant equations. The reader should consult Szabo and Ostlund's book for a more complete explanation [17,18].

Finally, one arrives at

$$\hat{f}\,\chi_i = \lambda_i \chi_i \qquad \text{i = 1,2,…….N} \qquad (2.30)$$

With

$$\hat{f}_i = -\frac{1}{2}\overrightarrow{\nabla_i^2} - \sum_{k=1}^{M}\frac{Z_k}{r_{ik}} + \sum_i^N\left[\widehat{J_j}\overrightarrow{x_i} - \widehat{K_j}\overrightarrow{x_i}\right] = \widehat{h_i} + \hat{V}^{HF}(i), \qquad (2.31)$$

the Fock operator for the i-th electron. In similarity to(2.26) to (2.29), the first two terms represent the kinetic and potential energy due to nucleus-electron interaction, collected in the core Hamiltonian $\widehat{h_\iota}$, whereas the latter terms are sums over the Coulomb operators $\widehat{J_J}$ and the exchange operators $\widehat{K_J}$with the other j electrons, which form the Hartree-Fock potential $\hat{V}^{HF}$ .There the major approximation of Hartree-Fock can be seen. The original Hamiltonian's two-electron repulsion operator is replaced by a one-electron operator, $\hat{V}^{HF}$ which describes average repulsion [17].

2.6 Limitations and failings of the Hartree-Fock approach

The number of electrons in an atom or a molecule might be even or odd. The compound is in a single state if the number of electrons is even and they are all in double occupied spatial orbitals ϕ_i Closed-shell systems are what they're called. Open-shell systems are compounds with an odd number of electrons and compounds with single occupied orbitals, i.e. species with a triplet or higher ground state. These two sorts of systems relate to two different Hartree-Fock techniques.

The restricted HF technique (RHF) considers all electrons to be paired in orbitals, whereas the unrestricted HF method (UHF) removes this restriction entirely. Open-shell systems can alternatively be described using an RHF approach, in which only the single occupied orbitals are eliminated, resulting in a limited open-shell HF (ROHF), which is more realistic but also more difficult and thus less popular than UHF [17].

The size of the investigated system can also be a limiting factor for calculations. Kohn states several $M = P^5$ with $3 \leq p \leq 10$ parameters for a result with us-cent accuracy in the investigation of the H_2 system [20]. For a system with N = 100 (active) electrons, the number of parameters rises to

$$M = P^{3N} = 3^{300} \text{ to } 10^{300} \approx 10^{150} \text{ to } 10^{300} \tag{2.32}$$

Equation (2.32) states, that the minimization of the energy would have to be performed in a space of at least 10^{150} dimensions which exceeds the computational possibilities nowadays by far. HF methods are therefore restricted to systems with a small number of involved electrons ($N \approx 10$). Referring to the exponential factor in (2.32) this limitation is sometimes called exponential wall [20].

The energy produced via HF calculations is always greater than the exact ground state energy because a multi-electron wave function cannot be captured entirely by a single Slater determinant. The Hartree-Fock-limit is the most precise energy obtained using HF methods [17].

The difference between E_{HF} and E_{xact} is called correlation energy and can be denoted as[21].

$$E_{corr}^{HF} = E_{min} - E_{HF} \tag{2.33}$$

Even though E_{corr} is usually small against E_{min}, as in the example of an N_2 molecule where

$$E_{corr}^{HF} = 14.9\text{eV} < 0.001 \cdot E_{min}, \tag{2.33}$$

It has the potential to have a significant impact[22].

The experimental dissociation energy of the N_2 molecule,

$$E_{dits} = 9.9\text{eV} < E_{corr} \tag{2.34}$$

This translates to a significant contribution of the correlation energy to relative energies like reaction energies, which are of special relevance in quantum chemistry.

The mean eld approximation utilized in the HF method contributes the most to the correlation energy. That is one electron moves in the average eld of the others, a method that ignores the fundamental correlation between electron movements. To better grasp what this means, consider electron repulsion at small distances, which is not addressed by a mean-field technique such as the Hartree-Fock method [17].

Chapter 3

Density functional theory

3.1 A new base variable - the electron density

A broad statement about the calculation of observables was provided in section 2.3, which dealt with the wave function ψ. The subject of this section is a quantity determined similarly. The basic variable in density functional theory is the electron density (for N electrons) [17, 23].

$$n(\vec{r}) = N \sum_{s1} \int d\overrightarrow{x_2} \dots \int d\overrightarrow{x_N}\, \Psi^*(\overrightarrow{x_1}, \overrightarrow{x_2} \dots, \overrightarrow{x_N}) \Psi(\overrightarrow{x_1}, \overrightarrow{x_2} \dots., \overrightarrow{x_N}) \qquad (3.1)$$

The notation in (3.1) takes into account a wave function that is dependent on spin and spatial coordinates. The integral in the equation indicates the chance of finding a specific electron with any spin in the volume element $d\overrightarrow{r_1}$ in more detail. Since the electrons are indistinguishable, N times the integral gives the probability that an electron is found there. The other electrons are represented by the wave function$\Psi(\overrightarrow{x_1}, \overrightarrow{x_2} \dots., \overrightarrow{x_N})$ have arbitrary spin and spatial coordinates [17].

If the spin coordinates aren't taken into account, the electron density can be described as a measurable observable that is just reliant on spatial coordinates [20, 23].

$$n(\vec{r}) = N \int d\overrightarrow{r_2} \dots \int d\overrightarrow{r_N}\, \Psi^*(\overrightarrow{r_1}, \overrightarrow{r_2} \dots, \overrightarrow{r_N}) \Psi(\overrightarrow{r_1}, \overrightarrow{r_2} \dots., \overrightarrow{r_N}) \qquad (3.2)$$

which can be determined, for example, using X-ray diffraction [17].

Before providing a method that uses electron density as a variable, make sure it has all of the relevant system information. That is to say, it must include information on the electron number N as well as the external potential, which is denoted by $\hat{V}$ [17].

Integrating the electron density over the spatial variables yields the total number of electrons [17].

$$N = \int d\overrightarrow{r_N}\ (\vec{r}). \tag{3.3}$$

What has to be demonstrated is that the electron density uniquely characterizes the external potential, up to a certain additive constant.

3.2 Thomas-Fermi Theory

One of the earliest tractable schemes for solving the many-electron problem was proposed by Thomas and Fermi [24, 25]. In this model, the electron density n(r) is the central variable rather than the wave function, and the total energy of a system is written as a functional E^{TF} [n(r)] where square brackets are used to enclose the argument of the functional, which in this case is the density. The Thomas-Fermi energy functional is composed of three terms,

$$E^{TF}[n(r)] = A_k \int n(r)^{5/3} dr + \int n(r) v_{ext}(r) dr + \frac{1}{2} \iint \frac{n(r)n(r\prime)}{|r-r\prime|}\, dr' \tag{3.6}$$

The first term is the electronic kinetic energy associated with a system of non-interacting electrons in a homogeneous electron gas. This form is obtained by integrating the kinetic energy density of a homogeneous electron gas t_0 [n(r)] [26, 27].

$$T^{TF}\ [n(r)] = \int t_0[n(r)]\ dr \tag{3.7}$$

Where t_0[n(r)] is obtained by summing all of the free-electron energy states $\varepsilon = \frac{K^2}{2}$, up to the Fermi wave vector $K_F = [3\pi^2 n(r)]^{\frac{1}{3}}$

$$t_0\ [n(r)] = \frac{2}{(2\pi)^3} \int \frac{K^2}{2} n_k dk = \frac{1}{(2\pi)^2} \int_0^k Fk^4 dk \tag{3.8}$$

NK is the density of allowed states in reciprocal-space. This leads to the form given in (3.9) with coefficient $A_k = \frac{3}{10}(3\pi^2)^{\frac{2}{3}}$. The power-law dependence on the density can also be established on dimensional grounds. The second term is the classical electrostatic energy of

attraction between the nuclei and the electrons, where $U_{ext}(r)$ is the static Coulomb potential arising from the nuclei,

$$U_{ext}(r) = - \sum_{j=1}^{M} \frac{Z_j}{|r-R_j|} \tag{3.9}$$

Finally, the third term in (3.8) represents the electron-electron interactions of the system, and in this case is approximated by the classical Coulomb repulsion between electrons, known as the Hartree energy.

To obtain the ground state density and energy of a system, the Thomas-Fermi equation (3.8) must be minimized subject to the constraint that the number of electrons is conserved. This type of constrained minimization problem, which occurs frequently within many-body methods, can be performed using the technique of Lagrange multipliers. In general terms, the minimization of a functional F[f], subject to the constraint C[f], leads to the following stationary condition

$$\delta(F[f] - \mu C[f]) = 0 \tag{3.10}$$

where μ is a constant known as the Lagrange multiplier. Minimizing (3.11) leads to the solution of the corresponding Euler equation,

$$\frac{\delta F[f]}{\delta f} - \mu \frac{\delta C[f]}{\delta f} = 0 \tag{3.11}$$

Applying this method to (3.7) leads to the stationary condition,

$$\delta \{ E^{TF}[n(r)] - (\int n(r)dr - N) \} = 0 \tag{3.12}$$

which yields the so-called Thomas-Fermi equations,

$$\frac{5}{3} A_k n(r)^{2/3} + v_{ext}(r) + \int \frac{n(r')}{[r-r']} dr' - \mu = 0 \tag{3.14}$$

that can be solved directly to obtain the ground state density, Thomas-Fermi theory suffers from many deficiencies, probably the most serious defect is that it does not predict bonding between atoms [28-30], so molecules and solids cannot form in this theory. The main source of error comes from approximating the kinetic energy in such a crude way. The kinetic energy represents a substantial portion of the total energy of a system and so even small errors prove disastrous. Another shortcoming is the over-simplified description of the electron-electron interactions, which are treated classically and so do not take account of quantum phenomenon such as the exchange interaction.

3.3 The Hohenberg-Kohn Theorems

The Hohenberg-Kohn theorems relate to any system consisting of electrons moving under the influence of an external potential $v_{ext}(r)$ Stated simply they are as follows:

Theorem 1: The energy functional E [n(r)] alluded to in the first Hohenberg-Kohn theorem can be written in terms of the external potential $v_{ext}(r)$ in the following way,

$$E\,[n(r)] = \int n(r)\, v_{ext}(r)\, dr + F\,[n(r)] \tag{3.15}$$

where F[n(r)] is an unknown but otherwise universal functional of the electron density n(r) only. Correspondingly, a Hamiltonian for the system can be written such that the electron wave function ψ that minimizes the expectation value gives the ground state energy (assuming a non-degenerate ground state),

$$E\,[n(r)] = \langle\psi|\hat{H}|\psi\rangle \tag{3.16}$$

The Hamiltonian can be written as,

$$\hat{H} = \hat{F} + \hat{V}_{ext} \tag{3.16}$$

where $\hat{F}$ is the electronic Hamiltonian consisting of a kinetic energy operator $\hat{T}$ and an interaction operator $\hat{V}_{ee}$,

$$\hat{F} = \hat{T} + \hat{V}_{ee} \tag{3.17}$$

The proof of the first theorem is remarkably simple and proceeds by *reductio ad absurdum*. Let there be two different external potentials, $v_{ext.1}(r)$ and $v_{ext,2}(r)$, that give rise to the same density $n_0(r)$. The associated Hamiltonians, $\hat{H}_1$ and $\hat{H}_2$, will therefore have different groundstate wave functions ψ_1 and ψ_2, that each yield $n_0(r)$. Using the variational principle [31]. together with (3.17) yields,

$$E_1^0 < \langle\psi_2|\hat{H}_1|\psi_2\rangle = \langle\psi_2|\hat{H}_2|\psi_2\rangle + \langle\psi_2|\hat{H}_1 - \hat{H}_2|\psi_2\rangle \tag{3.18}$$

$$= E_2^0 + \int n_0(r)[v_{ext,1}(r) - v_{ext,2}(r)] \tag{3.19}$$

where E_1^0 and E_2^0 are the groundstate energies of $\hat{H}_1$ and $\hat{H}_2$ respectively. It is at this point that the Hohenberg-Kohn theorems, and therefore DFT, apply rigorously to the ground state only.

An equivalent expression for (3.20) holds when the subscripts are interchanged. Therefore adding the interchanged inequality to (3.21) leads to the result:

$$E_1^0 + E_2^0 < E_2^0 + E_2^0 \tag{3.20}$$

which is a contradiction, and as a result, the groundstate density uniquely determines the external potential $v_{ext}(r)$, to within an additive constant. Stated simply, the electrons determine the positions of the nuclei in a system, and also all groundstate electronic properties, because as mentioned earlier $v_{ext}(r)$ and N completely define $\widehat{H}$.

Theorem 2:

The ground state energy can be obtained variationally: the density that minimizes the total energy is the exact ground-state density.

The proof of the second theorem is also straightforward: as just shown, n(r) determines $v_{ext}(r)$, N and $v_{ext}(r)$ determine $\widehat{H}$ and therefore ψ. This ultimately means ψ is a functional n(r) of, and so the expectation value of $\hat{F}$ is also a functional of n(r) , i.e.v

$$F\,[n(r)] = \langle\psi|\hat{F}|\psi\rangle \tag{3.20}$$

A density that is the ground-state of some external potential is known as v-representable. Following from this, a v-representable energy functional $E_u[n(r)]$ can be defined in which the external potential v(r) is unrelated to another density n′ (r)

$$E_v[n'(r)] = \int n'(r)\, v_{ext}(r)\, dr + F\,[n'\,(r)] \tag{3.21}$$

and the variational principle asserts,

$$\langle\psi'|F\hat{}\,|\psi'\rangle + \langle\psi'|\hat{V}_{ext}|\psi'\rangle > \langle\psi|\hat{F}|\psi\rangle + \langle\psi|\hat{V}_{ext}|\psi\rangle \tag{3.22}$$

where ψ is the wave function associated with the correct groundstate n(r). This leads to,

$$\int n'(r)\, v_{ext}(r)\, dr + F\,[n'\,(r)] > \int n(r)\, v_{ext}(r)\, dr + F\,[n(r)] \tag{3.23}$$

and so the variational principle of the second Hohenberg-Kohn theorem is obtained,

$$E_v[n(r)] > E_v\,[n(r)] \tag{3.24}$$

Although the Hohenberg-Kohn theorems are extremely powerful, they do not offer a way of computing the ground-state density of a system in practice. About one year after the seminal

DFT paper by Hohenberg and Kohn, Kohn and Sham [20] devised a simple method for carrying out DFT calculations that retains the exact nature of DFT.

3.4 Kohn-Sham Equations

While the Hohenberg-Kohn theorem indicates that the ground state density can be used to compute system attributes, it does not show how to find the ground state density. The Kohn-Sham equations [32] propose a way to get there. Consider the ground state energy as a function of the charge density to get these equations.

$$E\,[\rho(r)] = T[\rho(r)] + \int \rho(r)\, v(r) dr + E_{ee} \tag{3.25}$$

The kinetic energy is the first term in (3.25), followed by the interaction with the external potential, which includes the electron-nuclei interaction, and finally, the electron-electron interaction, which can be represented as

$$E_{ee}[\rho(r)] = \frac{1}{2} \int \frac{\rho(r)\rho(r\prime)}{[r-r\prime]}\, dr\, dr' + E_{xc}\,[\rho(r)] \tag{3.26}$$

The electron-electron electrostatic interaction is the first term on the right-hand side of (3.26), while the non-classical exchange-correlation energy is the second. By reintroducing wave functions ψ_i with new values, Kohn and Sham were able to generate a set of single-particle SEs.

$$\rho(r) = \sum_{i=1}^{n} \psi_i^*(r)\, \psi_i(r) \tag{3.27}$$

where n is the number of electrons. The kinetic energy is given by

$$T[\rho(r)] = -\frac{\hbar^2}{2m} \sum_i^n \langle \psi_i | \nabla^2 | \psi_i \rangle \tag{3.28}$$

If the wave functions must be orthonormal, i.e.,

$$\int \psi_i^*(r) \psi_j(r) dr = \delta_{ij} \tag{3.29}$$

then we can define a function of the wave functions

$$\Omega[\psi_i] = E\,[\rho(r)] - \sum_i \sum_j \epsilon_{ij} \int \psi_i^*(r) \psi_j(r) dr \tag{3.30}$$

where ϵ_{ij} are Lagrange multipliers to ensure the wavefunctions are orthonormal. Minimization of $\Omega[\psi_i]$ concerning $\psi_i^*(r)$ gives the Kohn-Sham equations

$$[-\frac{\hbar^2}{2m}\nabla^2+\nu_{eff}(r)]\,\psi_i(r) = \epsilon_i\psi_i(r) \tag{3.31}$$

$$\nu_{eff}(r) = \nu(r) + \int \frac{\rho(r\prime)}{[r-r\prime]}\, dr' + \nu_{xc}(r) \tag{3.32}$$

Where $\nu_{xc}(r)$ is the exchange-correlation potential given by

$$\nu_{xc}(r) = \frac{\delta E_{xc}}{\delta\rho(r)} \tag{3.33}$$

A unitary transform is used to ensure that the wave functions $\phi_i(r)$are orthonormal while transitioning from (3.30) to (3.31) [33]. As can be observed, (2.15) has the same structure as the Schrödinger equation for a single particle with an effective local potential ν_{eff} defined in (2.16). This is in contrast to the Hartree-Fock equations [34], in which the one-electron equations have a non-local potential.

A well-known method for solving the Kohn-Sham equations is to start with an initial trial electron density, as shown in Figure 3.1. Calculate these equations using the trial electron density. After solving the Kohn-Sham equations, we will have a set of single electron wave functions. These wave functions can be used to calculate the new electron density. As an input, the new electron density is fed into the next cycle. Finally, after each iteration, compare the differences in calculated electron densities. If the difference in electron density between consecutive iterations is less than a suitably determined convergence threshold, the solution of the Kohn-Sham equations is deemed self-consistent. The predicted electron density has now been converted to the ground state electron density, which can be used to compute the total energy of the system [29].

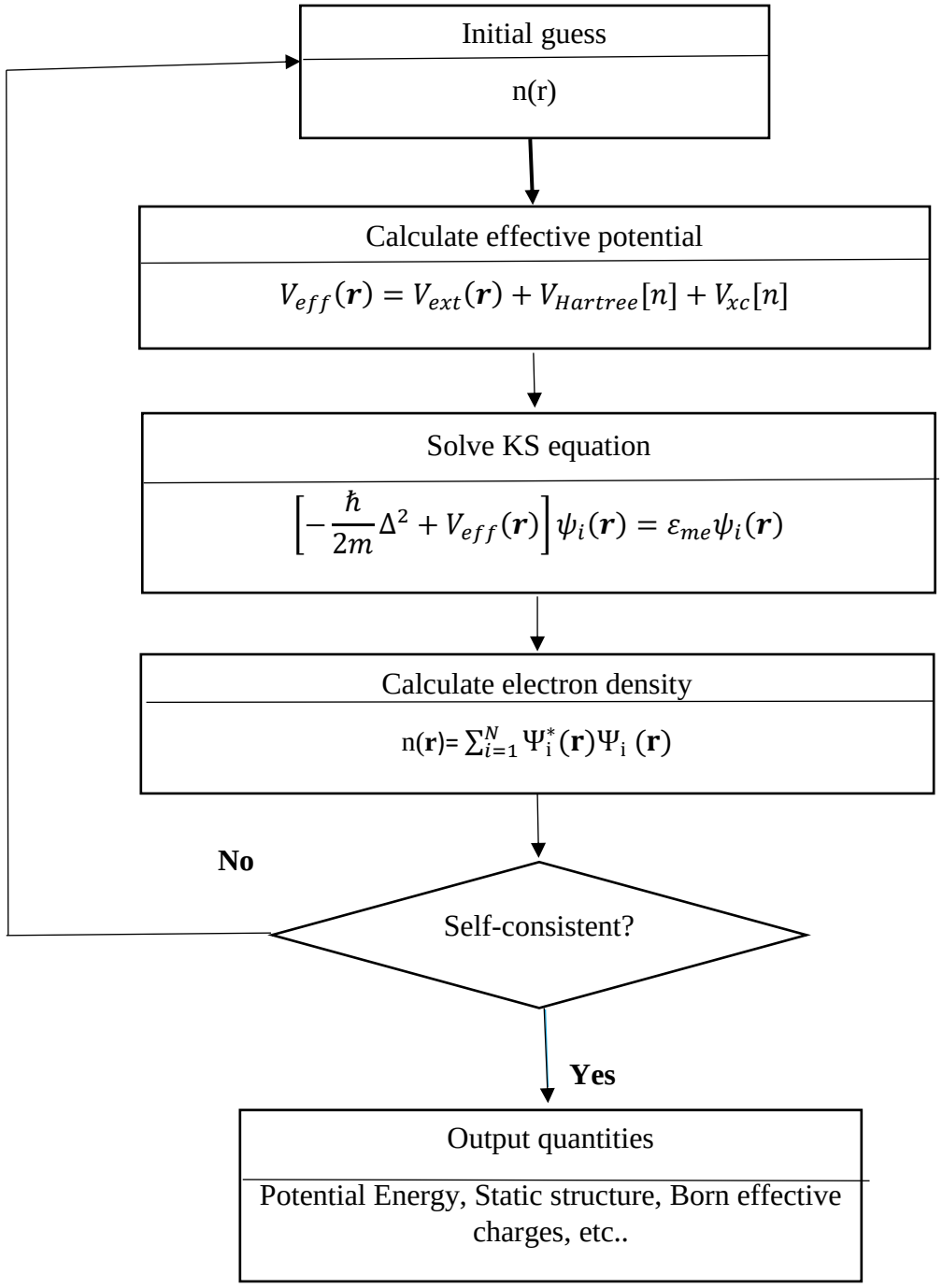

Figure 3.1: Illustration of the self-consistent field (SCF) procedure for solving the Kohn-sham equations.

3.5 The Exchange-Correlation Functionals

Because the true shape of the exchange-correlation functional is unknown, it's difficult to solve the Kohn-Sham equations. Two basic approximation methods have been implemented to approximate the exchange-correlation functional. The local density approximation (LDA) is

the first effort to estimate the exchange-correlation functional in DFT computations. The second well-known class of approximations to the Kohn-Sham exchange-correlation functional is the generalized gradient approximation (GGA). In the GGA approximation, the local electron density and local gradient in the electron density are included in the exchange and correlation energies [35].

3.6 Local Density Approximation (LDA)

The local density approximation is the simplest approximation to the exchange-correlation functional (LDA). The energy density of a homogeneous electron gas with the same electron density r at every site in the molecule has the value that would be supplied by a homogeneous electron gas with the same electron density r at that point, according to the local density approximation. The term "local" was coined to distinguish the technique from those in which the functional is reliant not only on r but also on the gradient (first derivative) of r, with the distinction arising from the assumption that a derivative is a nonlocal characteristic. Local spin density approximation (LSDA; see below) functionals, which are an extension of the LDA technique, have largely replaced LDA functionals [36].

As a practical approximate expression for $E_{xc}[n]$, Kohn and Sham suggested what is known in the context of DFT as the local density approximation, or LDA:

$$\mathrm{E_{xc}[n(r)]} \simeq \int \mathrm{drn(r)}\epsilon_{\mathrm{xc}}\big(\mathrm{n(r)}\big) \tag{3.34}$$

Where $\epsilon_{xc}(n)$ is the exchange-correlation energy per electron in a uniform electron gas of density n. this quantity is known exactly in the limit of high density and can be computed accurately at densities of interest, using Monte Carlo techniques.

The addition of the potential is the only difference between the resulting computational strategy and a naive mean-field approach.

$$\boldsymbol{v_{xc}(r) = \frac{d(n\epsilon_{xc}(n)}{dn}} \tag{3.35}$$

At the relevant stage in the self-consistency loop, to the electrostatic potential. The ground state energy has the following expression:

$$E_0 = \sum_{i=1}^{N} \epsilon_i - E_{es}[n(r)] + \int dr\, n(r)(\epsilon_{xc}\big(n(r)\big) - v_{xc}\big(n(r)\big) \tag{3.36}$$

The first component is the noninteracting energy, the second term is half of the Hartree scheme's double-counting of the electrostatic energy, and the third term is a similar subtraction for the exchange-correlation energy [37]. When the density is slowly changing, the local approximation is only valid in a theoretical sense. LDA delivers very good results even though atom and molecule densities are often highly inhomogeneous. LDA has been found to produce relatively satisfying findings for equilibrium structures, harmonic frequencies, and dipole moments in molecules [38].

3.7 Generalized-Gradient Approximation (GGA)

In many circumstances, the creation of multiple generalized-gradient approximations (GGAs) that include density gradient corrections and larger spatial derivatives of the electron density outperforms LDA. Becke (B88), Perdew, et al, and Perdew, Burke, and Enzerhof are three of the most extensively utilized GGAs (PBE). The definition of the XC energy functional of GGA is the generalized form of LSDA to include corrections from density gradient $n(r)$as

$$E_{XC}^{GGA}[n_{\uparrow}(r), n_{\downarrow}(r)] = \int n(r)\epsilon_{XC}^{hom}(n_{\uparrow}(r), n_{\downarrow}(r), |\nabla n_{\uparrow}(r)|, |\nabla n_{\downarrow}(r)|, \dots\dots)dr$$

$$= \int n(r)\epsilon_{XC}^{hom}\big(n(r)\big)F_{XC}\,(n_{\uparrow}(r), n_{\downarrow}(r), |\nabla n_{\uparrow}(r)|, |\nabla n_{\downarrow}(r)|, \dots)d \quad (3.37)$$

Where F_{XC} is dimensionless and $\epsilon_X^{hom}(n(r))$ is the exchange energy density of the unpolarized HEG. F_{XC} Can be decomposed linearly into exchange contribution F_X and correlation contribution F_C as $F_{XC} = F_X + F_C$. For a detailed treatment of F_X and F_C indifferent GGAs. GGA beats LDA in forecasting molecular bond length and binding energy, crystal lattice constants, and other parameters in general, especially in systems with rapidly changing charge density. When the lattice constants from LDA calculations match actual data well, but GGA overestimates it, GGA overcorrects LDA results in ionic crystals [39].

Chapter 4

Results and discussion

4.1 Crystallographic structure

The atomic position and space group information about the $RbInX_3$ (X= Cl, Br) compound in the unit cell were taken from ref [40] with the space group 221_Pm-3m. $RbInX_3$ (X= Cl, Br) is a perovskite-type compound crystallizing in a cubic system.

Table 4.1: Optimized lattice parameters and Wyckoff positions for cubic $RbInX_3$ (X = Cl, Br).

Perovskite Compounds	Optimized Lattice Parameters (Å)	Wyckoff Positions			
		Atom	X	Y	Z
$RbInCl_3$	5.4621	Rb	0	0	0
		In	0.5	0.5	0.5
		Cl_3	0.5	0.5	0
$RbInBr_3$	5.7430	Rb	0	0	0
		In	0.5	0.5	0.5
		Br_3	0.5	0.5	0

We are performed for all the studied compounds. Gained optimized lattice parameters along with the available theoretical parameters and Wyckoff positions are collated in Table 4.1

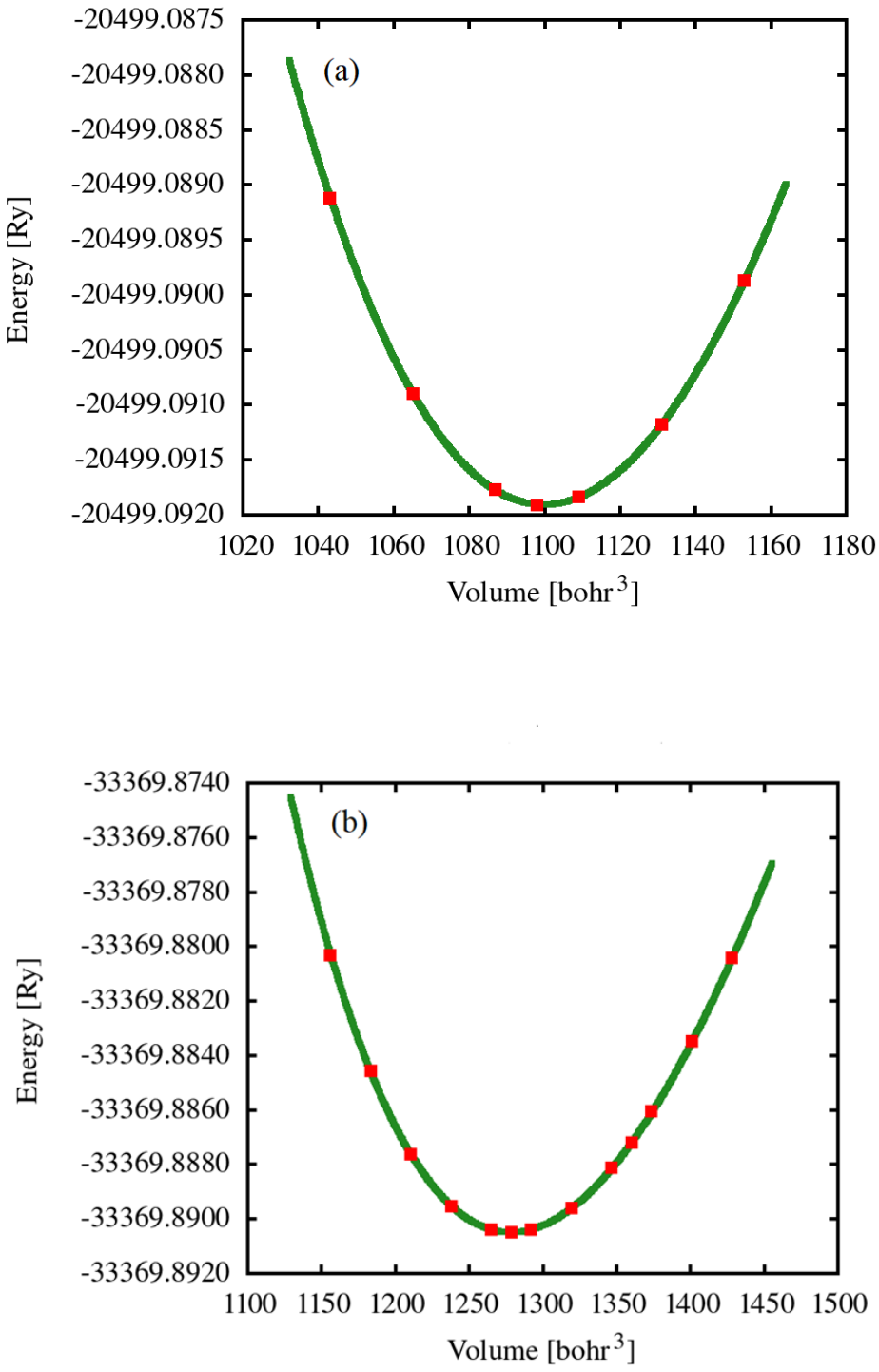

Figure. 4.1. Energy v/s volume optimization curves for (a) $RbInCl_3$ and (b) $RbInBr_3$.

The optimized lattice parameters for RbInX3 (X = Cl, Br) are in a close agreement given the theoretical values provided, confirming the accuracy of the calculations. These parameters are then used to compute the desired attributes of the materials being researched. As mentioned above in WIEN2k software, we ran volume optimization calculations for each potential to obtain the best theoretical lattice parameters, which are the closest to experimental value and gave the minimum Energy value (Figure 1). So, Energy v/s volume optimization curves are plotted for all compounds, and results for more responsive $RbInX_3$ (Cl, Br) are presented in Figure. 1(a, b).

The values of radius of muffin-tin (RMT) spheres for atoms were taken to be 2.5 a.u. Major, plane wave functions were distended up to $R_{MT} \times K_{MAX} = 8.5$, where 'RMT' represents the radius of muffin-tin (MT) radius of the non-overlapping atomic sphere which is the smallest size neutral atoms, and 'KMAX' represents the largest value of the reciprocal lattice vector[33]. Other variables that are taken into account in the current computations are GMAX = 12.0 (a.u.) l_{max} = 10.0, 1000 k point To ensure that the computations are correct, cutoff values for energy, forces, and core and valence state's separation were kept as 0.0001 Ry(Energy convergence), 1 mRy/a.u and − 6.0 Ry, respectively.

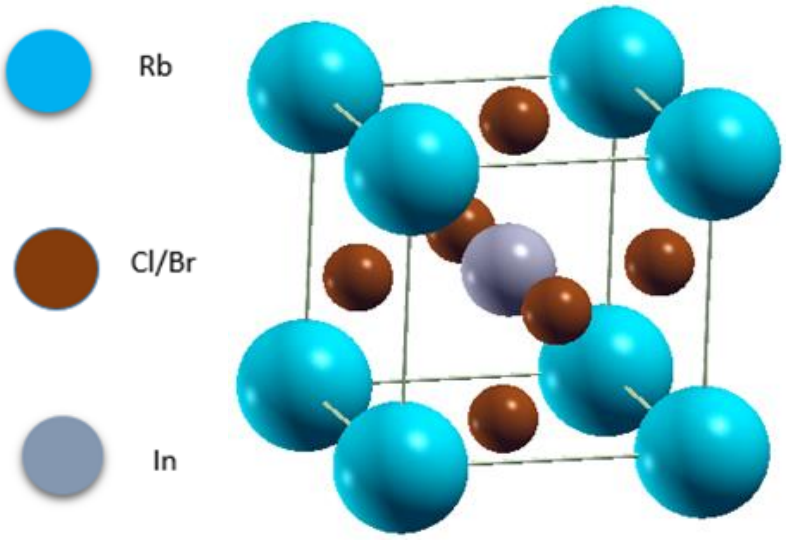

Figure 4.2: Crystal structure of $RbInX_3$ (X=Cl, Br)

4.2 Self Consistent Field (SCF) Calculation

We generated the structure using the optimized lattice parameters after volume optimization, and then we initialized it for SCF calculation. Self-consistent field (SCF) methods include both

Hartree-Fock (HF) theory and Kohn-Sham (KS) density functional theory (DFT). Self-consistent field theories only depend on those that are specific to DFT can be found in Density functional theory (DFT) [20].

We got the same Exchange- correlation potential as PBE-GGA both perovskite compound $RbInX_3$ (X=Cl, Br) and GAP = 0.0 eV Where K- mesh details are 1000k. The parameters we used for SCF calculation are listed below in table 4.2 and results showing below the table 4.3 after SCF calculation

Table 4.2: Parameter used in SCF calculation of $RbInX_3$ (X=Cl, Br) material.

Compounds	Optimized Lattice Parameters(Ry)	RK_{max}	K-point	Convergence Citeria	
				Energy(Ry)	Charge (e)
$RbInCl_3$	5.4621	8.5	1000	0.00001	0.0001
$RbInBr_3$	5.7430	8.5	1000	0.00001	0.0001

Table 4.3: Calculated Total Energy(Ry) and Fermi Energy (eV).

Compounds	Exchange correlation-potential	Total Energy (Ry)	Fermi Energy (eV)
$RbInCl_3$	PBE-GGA	-20499.09189789	0.1505896542
$RbInBr_3$	PBE-GGA	-33369.8904861	0.1334087524

4.3 Bandstructure

Band structure calculations take advantage of the periodic nature of a crystal lattice, exploiting it is symmetry. The bandgap is the energy difference between the lowest point of the conduction band and the highest point of the valance band Figure 03 (a, b) shows the Energy band structure using PBE-GGA functional. From the figure, we can see there is no bandgap of 0.0 eV. In a metal, there is no band gap between the valance band and conduction band. The conduction band crosses the Fermi level and enters into the valance band. Although, in some metals, the conduction and valance bands partially overlap. This means that electrons can move freely between the conduction and valance band. In a metal, the Fermi level is inside of one or more allowed bands. The Fermi energy level is distinguished with a solid line at 0 eV. The top point

of the valance band and bottom point of the conduction band is at 0 eV in the PBE-GGA band structure. Since the Fermi level in metal is at absolute zero the energy of the highest occupied single-particle state.

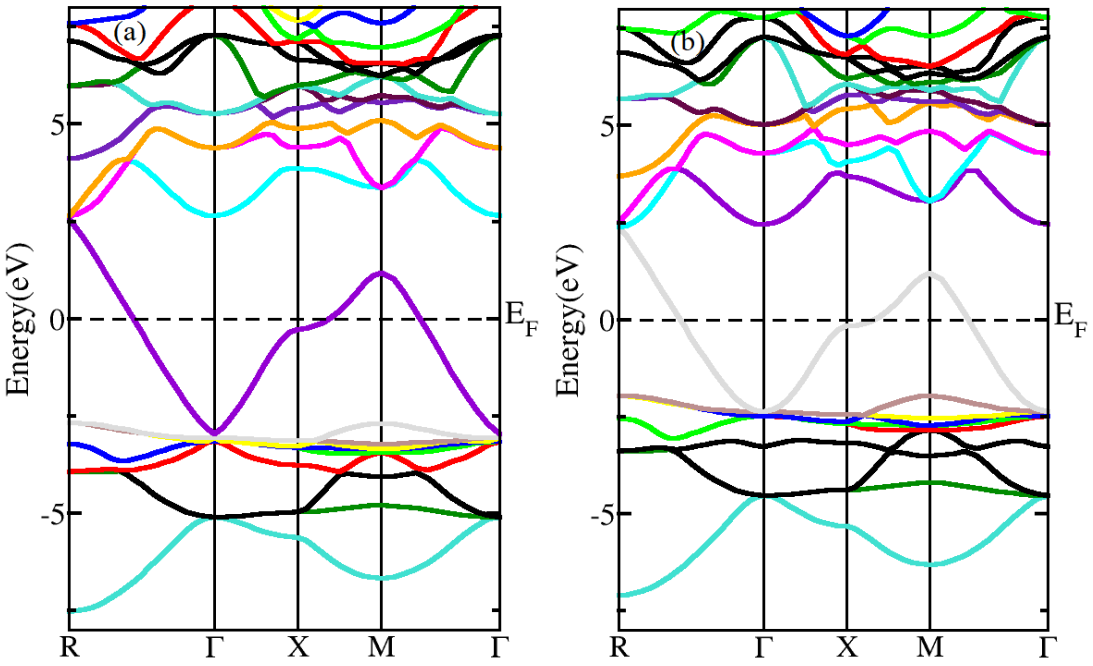

Figure 4.3: Band structure plotted for (a) $RbInCl_3$ (b) $RbInBr_3$

4.4 Density of state

The density of states (DOS) is essentially the number of different states at a particular energy level that electrons are allowed to occupy, i.e. the number of electron states per unit volume per unit energy. DOS calculations allow one to determine the general distribution of states as a function of energy and can also determine the spacing between energy bands [41]. Also, the Density of state describes the probability of electron distribution in the energy spectrum.

A DOS of zero means that no states can be occupied at that energy level. The total density of states (DOS) is more descriptive of the electronic nature of $RbInX_3$ (X=Cl, Br) compounds. Figure 4.4 shows the calculated DOS where the latter establishes the contribution of each atom to DOS. From the below Figure 4.4, the conduction band overlaps the fermi level and enters into the valence band region. DOS contribution in the valance band region is higher than the conduction band. We get the higher peak of DOS in the valance band region. In $RbInX_3$ (X=Cl,

Br) systems, the Cl atom contribution in the DOS is higher than the other atoms. The Rb atom contribution is very low in the valance band than the conduction band.

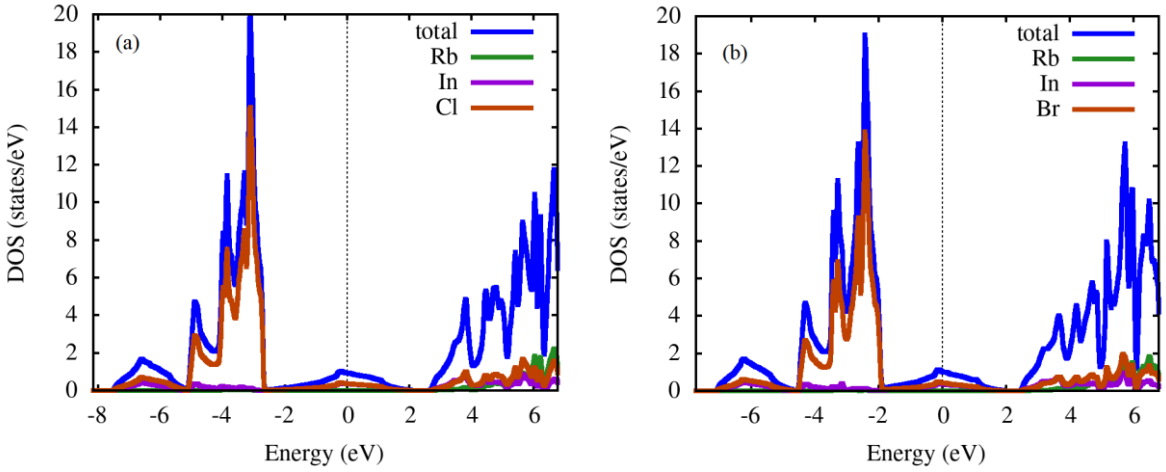

Figure 4.4: Total density of states plotted for (a) $RbInCl_3$ (b) $RbInBr_3$

4.5. Optical Properties

The optical properties of a material determine how it interacts with light. Some optical properties of $RbInX_3$ (X=Cl, Br) will be explored in this section. We were using plasma frequency typically 2.8973 eV and 2.8412 eV for $RbInX_3$ (X=Cl, Br).

4.5.1 Absorption coefficient

Basically, absorption coefficients are the measure of light that might be absorbed by a given thickness of a material. We calculate the optical absorption spectra for $RbInX_3$(X=Cl, Br) using PBE functional. Figure 5 represents the absorption coefficient versus energy for PBE functional and indicates significant absorption in the visible energy range (0–14 eV). It was also noticed that the graph is showing a strange trend that is. Initially, it decreases, and then it goes to increase. The visible range of light is 1.8 eV to 3.4 eV. In the visible region, the absorption coefficient is almost zero. That means that $RbInX_3$ (X=Cl, Br) compounds cannot be visible light. After the visible light region the absorptivity increases we got a sharp peak between 11.8

– 14 eV for RbInCl3and 10.8 – 14 eV for $RbInBr_3$. Here is the result we can see that two lines one is for $RbInCl_3$ and $RbInBr_3$. This material acts as a good absorber.

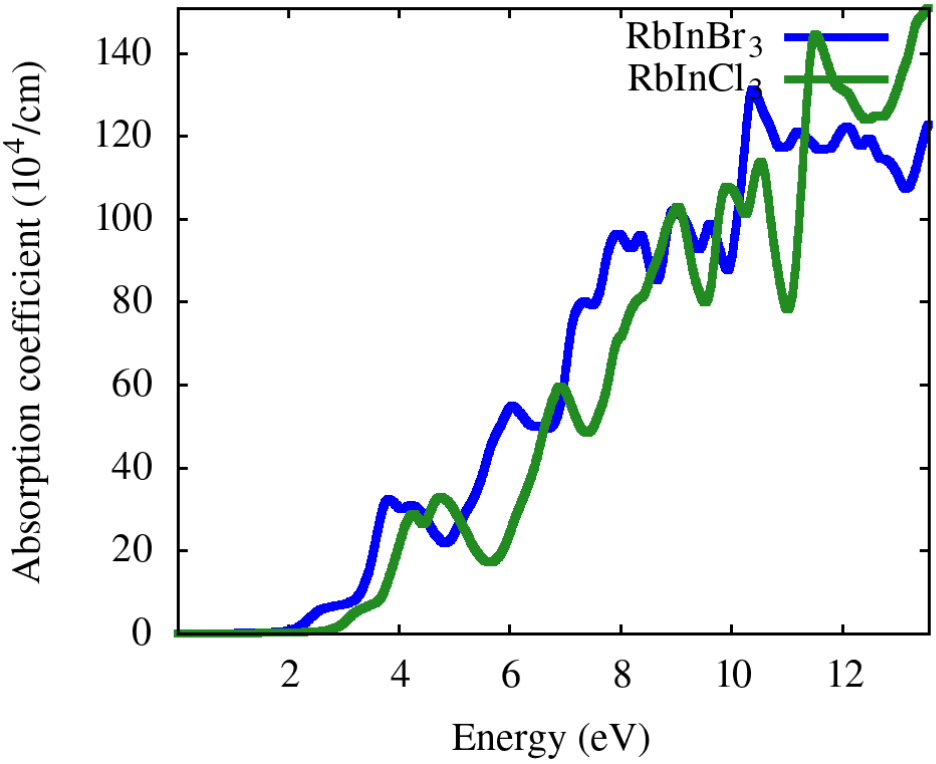

Figure 4.5: Absorption coefficient for $RbInX_3$ (X=Cl, Br)

4.5.2 Optical conductivity

Optical conductivity is a very important property to measure the electronic states of a material. It is closely related to dielectric function. It depends upon optical band gap, refractive index, absorption coefficient, incident photon frequency, extinction coefficient. Figure 6 shows the optical conductivity at different energy. The optical conductivity is the extension of electrical transport to high frequency. The maximum value of optical conductivity of the compound is obtained at 11.8 eV for $RbInCl_3$ and another direction for $RbInBr_3$ displays the maximum value of optical conductivity of the compound is obtained at 10.8 eV. Both plot shows, initially optical conductivity is almost zero. As light energy approached, it started to increase and maximum optical conductivity was noticed that both compounds. After reaching this stage it again decreases.

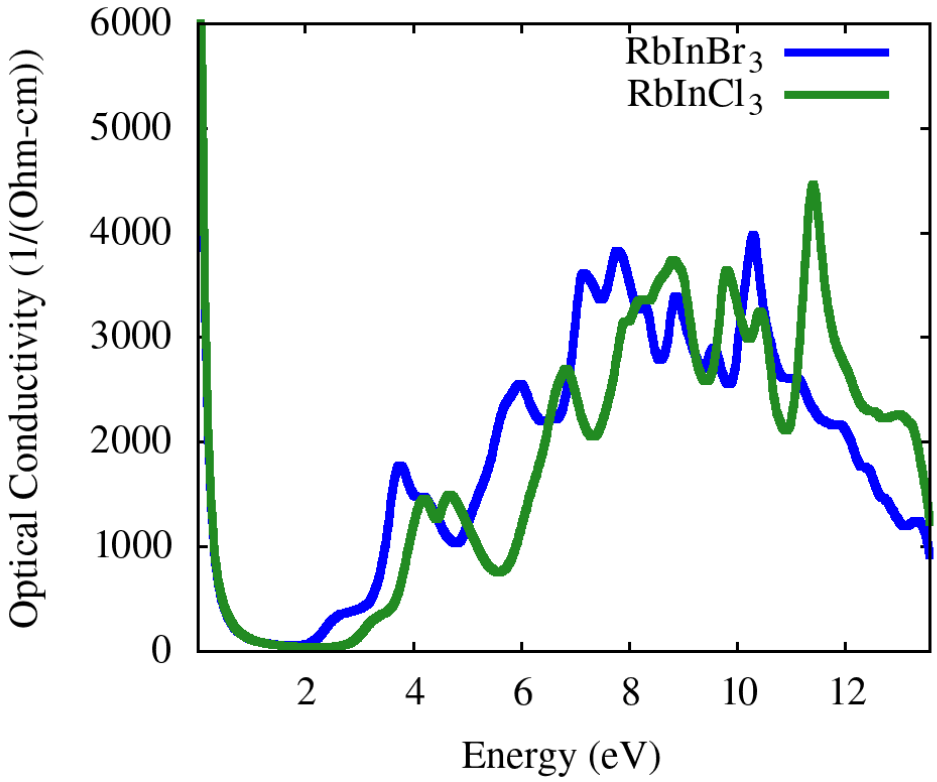

Figure 4.6: Optical conductivity for $RbInX_3$ (Cl, Br).

4.5.3 Refractive index

Refractive index is the measurement of how light propagates through a material. Higher the refractive index, slower will light travels through the material that changes its direction. It is very essential optical constant and plays an important role in designing the optical device. The refractive index versus the incident photon energy is shown in Figure 07. It should be noted that the refractive index is directly proportional to the magnetic moment of the system, which shows the dependency of the refractive index to their magnetic properties of them. We observe the optically isotropic nature of this compound in the lower energy range. For lower energies, the refractive index value is almost constant and as the energy increases, it attains a maximum value and exhibits decreasing tendency for higher energy values. The static refractive index is found to have the value typically 30 for $RbInCl_3$ and zero for $RbInBr_3$.

The refractive index is greater than one because as photons enter a material they are slowed down by the interaction with electrons. The more photons are slowed down while traveling through a material, the greater the material's refractive index. Generally, any mechanism that increases electron density in material also increases the refractive index

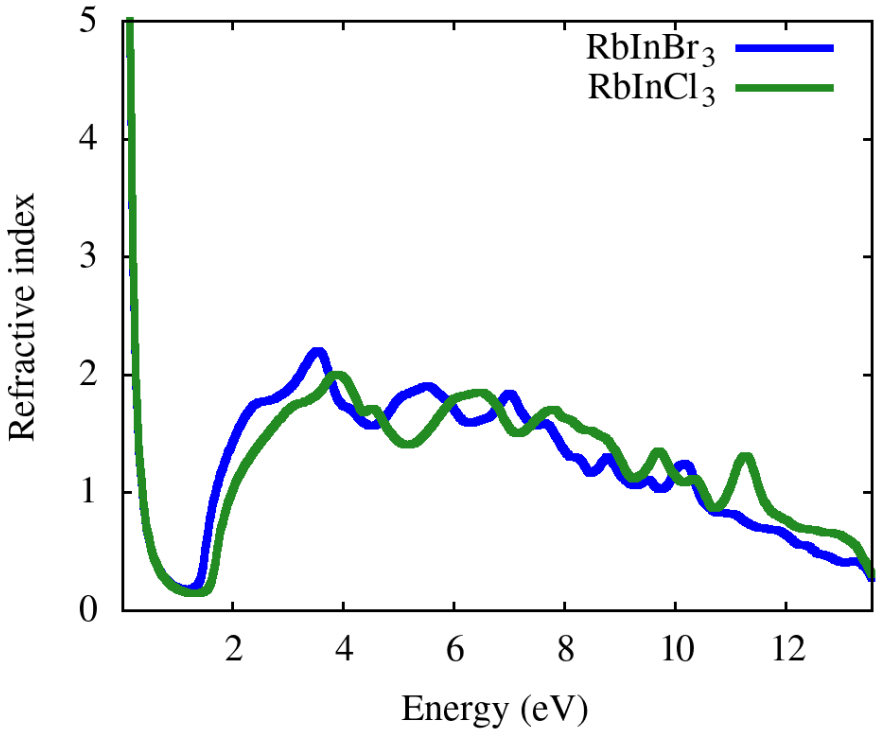

Figure 4.7: Refractive index for $RbInX_3$ (X=Cl, Br)

4.5.4: Optical Reflectivity

Reflectivity is an optical property of material, which describes how much light is reflected from the material with an amount of light incident on the material. The optical reflectivity R (ω) is displayed in Fig 08 we see that at zero position energy the reflectivity is highest but after 0 eV position reflectivity starts to decrease and becomes zero at the 1.9 eV and 2 eV respectively. After both positions, the reflectivity again increases. As the energy increases the reflectivity also increases. In both property observations, we can say that $RbInCl_3$ and $Rbinbr_3$ are good metallic reflectors.

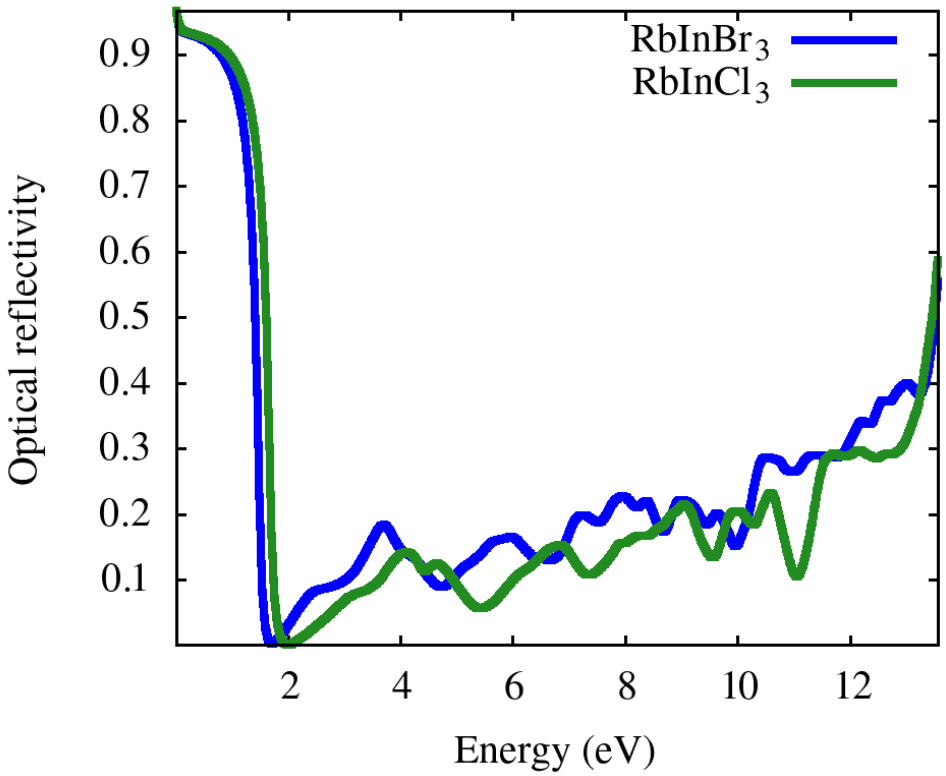

Figure 4.8: Optical reflectivity for $RbInX_3$ (X=Cl, Br)

4.5.5 Dielectric Tensor

The optical properties of the perovskites can be described by the electronic dielectric function $\varepsilon(\omega)$. The most relevant frequency-dependent complex dielectric function $\varepsilon(\omega)$ is studied to explore the optical impedance of the medium during the electromagnetic interaction. The dielectric function $\varepsilon(\omega)$ describes the optical response of the medium to the incident photons with an energy $E = \hbar\omega$. In terms of the complex dielectric function $\varepsilon(\omega)$, the dielectric function of an anisotropic material can be expressed as;

$$\varepsilon(\omega) = \varepsilon_1(\omega) + i\varepsilon_2(\omega)$$

where $\varepsilon_1(\omega)$ and $i\varepsilon_2(\omega)$ are the real and imaginary components of the dielectric function, respectively [42]. It's worth noting that the real and imaginary components of $\varepsilon(\omega)$ correspond to the quantity of energy stored in any medium and the amount of energy lost during solar absorption, respectively. Fig09 represents the real $\varepsilon_1(\omega)$ and the imaginary $\varepsilon_2(\omega)$ parts of the dielectric function, which depends on the frequency, for $RbInX_3$ (Cl, Br).

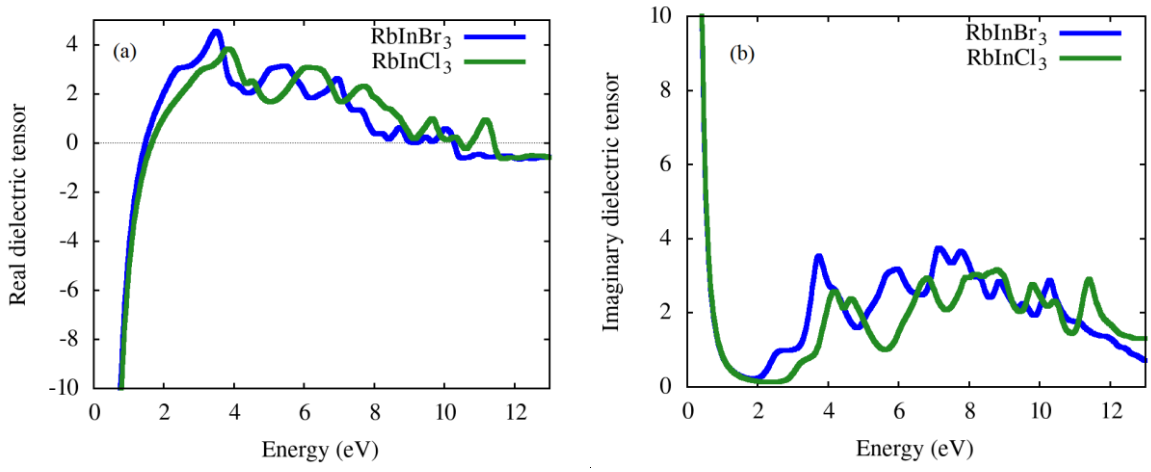

Figure 4.9: Dielectric tensor for $RbInX_3$ (X=Cl, Br) (a) Real and (b) Imaginary

The imaginary part of the dielectric function indicates absorption limits of the materials and energy gain ability as solar cells. The real part indicates the energy store ability of the material. Let us divide the curve into two main regions: a low energy region and a high energy region. From the real part of dielectric function $\varepsilon_1(\omega)$, the dielectric constant values can be found for any frequency. From fig 09 real part both compounds and the imaginary part both compounds obtained from PBE-GGA potential give the same graph. Real and imaginary parts of the dielectric constant are displayed in Figures 9 a and b for the RbInX3 (X=Cl, Br) compound. The value of the static real part of the dielectric function $\varepsilon_1(\omega)$ for the RbInX3 (X=Cl, Br) compound Figure 9a is negative, while the imaginary part of the static dielectric function $\varepsilon_2(\omega)$ Figure 9b is positive; this implies two important facts: Firstly, the $RbInX_3$ (X=Cl, Br) compound has considerable metallic behavior, which agrees with the energy band structure calculations. Secondly, the negative value of (ε_1) especially in the energy range 0–1.15 eV in Figure 9a, and the highly positive value of $\varepsilon_2(\omega)$ at the early beginning of Figure 9b, reveal the loss of light transit.

4.6 Elastic Properties

The mechanical characteristics of $RbInX_3$ (Cl, Br) are investigated using elastic constant calculations. The nature of the bonding forces and mechanical stabilities is influenced by elastic constants. Elastic constants are fundamental properties of solid materials. The propagation of

an elastic wave through a medium depends on the elastic constants of that material. From the strain as a function of volume, the elastic constants C_{11}, C_{12} were determined. The IRelast package, as implemented in WIEN2k, is used to examine elastic constant in this report. The following are the born stability conditions for cubic crystal [43-45]. Born stability criteria for cubic crystals are given as [46, 47].

$$(C_{11}\text{-}C_{12}) > 0,\ C_{11}>0,\ C_{44}>0,\ (C_{11} + 2C_{12})>0$$

The estimated elastic constants satisfy the Born stability criterion, and these elastic constants are listed in table 4. C_{11} represent in X-direction under linear compression [48]. For both studied compounds, the value of C_{12} is negative, which shows the decrease in transverse expansion when stress is applied. From elastic constants (C_{11}, C_{12}), we can easily calculate the elastic moduli, bulk modulus (B), by using Voigt-Reuss-Hill approximation [49].

$$B = \frac{1}{3}\ (C_{11} + 2C_{12}) \qquad 4.6.1$$

Bulk modulus calculates the resistance to volume changes under pressure [50] and can easily be calculated from Equation (4.6.1) by using elastic constants. Calculate elastic constant, C_{11} and C_{12} (in GPa) are 54.2803, 14.9489 respectively. Also, calculate the value of the bulk modulus of 28.059 GPa.

Chapter 05

Conclusions

The various properties of $RbInX_3$ (X= Cl, Br) compounds were studied. In this work, we have studied the structural, elastic, electronic, and optical properties of the cubic perovskite using the utmost precise full-potential linearized augmented plane wave (FP-LAPW) method as embodied in WIEN2k code within the generalized gradient approximation (GGA) in the framework of density functional theory (DFT). From band structure calculation, it is found that both compounds exhibit metallic behavior with no bandgap structure. The optical properties such as real and imaginary dielectric function, reflectivity, absorption coefficient, the real part of optical conductivity, refractive index are studied in the energy range of 0 to14 eV. The elastic properties have been investigated, which followed the Born stability criteria. Several mechanical properties, like Bulk modulus, Young's modulus, shear modulus, and anisotropy factor were computed by using the values of Cij. The elastic constants (C_{11}, C_{12}), bulk modulus are also calculated and discussed. The material $RbInCl_3$ showed the value of bulk modulus of 28.059 GPa.

Bibliography

References

[1] "S.V. Melnikova, A.T. Anistratov, B.V. Beznosikov, Sov. Phys. Solid State 19, 1266 (1977."

[2] P. C. Reshmi Varma, "Chapter 7 - Low-Dimensional Perovskites," S. Thomas and A. B. T.-P. P. Thankappan, Eds. Academic Press, 2018, pp. 197–229.

[3] "A. Szabo and N.S. Ostlund. Modern Quantum Chemistry. McGraw-Hill, 1989."

[4] "Blaha, P.; Schwarz, K.; Sorantin, P.; Trickey, S.B. (1990). 'Full-potential, linearized augmented plane wave programs for crystalline systems'. Computer Physics Communications. 59 (2): 399–415. Bibcode:1990CoPhC..59..399B. doi:10.1016/0010-4655(90)90187-6."

[5] "Schwarz, Karlheinz; Blaha, Peter (2003). 'Solid-state calculations using WIEN2k'. Computational Materials Science. 28 (2): 259–273. doi:10.1016/S0927-0256(03)00112-5."

[6] M. Sigrist, B. Cummings, D. Gruyter, A. Verlagsgesellschaft, H. Deutsch, and A. Wesley, "Inhaltsverzeichnis," vol. 13, pp. 1–113, 2003.

[7] E. Schrödinger, "An Undulatory Theory of the Mechanics of Atoms and Molecules," *Phys. Rev.*, vol. 28, no. 6, pp. 1049–1070, Dec. 1926, DOI: 10.1103/PhysRev.28.1049.

[8] B. de Wit, J. Hoppe, and H. Nicolai, “On the quantum mechanics of supermembranes,” *Nucl. Physics, Sect. B*, vol. 305, no. 4, pp. 545–581, 1988, DOI: 10.1016/0550-3213(88)90116-2.

[9] W. Pauli, “The Connection Between Spin and Statistics,” *Phys. Rev.*, vol. 58, no. 8, pp. 716–722, Oct. 1940, DOI: 10.1103/PhysRev.58.716.

[10] A. Jabs, “Connecting spin and statistics in quantum mechanics *,” *arXiv.org*, vol. arXiv:0810, Feb. 2014.

[11] W. PAULI, “On the Connexion between the Completion of Electron Groups in an Atom with the Complex Structure of Spectra,” *Old Quantum Theory*, pp. 184–203, 1967, DOI: 10.1016/b978-0-08-012102-4.50019-x.

[12] N. Zettili, “Quantum Mechanics Concepts and Applications Second Edition Library of Congress Cataloging-in-Publication Data,” [Online]. Available: www.wiley.com.

[13] K. Capelle, “A bird’s-eye view of density-functional theory,” *Braz. J. Phys.*, vol. 36, Dec. 2002, DOI: 10.1590/S0103-97332006000700035.

[14] L. zur T. P. I, “T. Flieÿbach. Mechanik: Lehrbuch zur Theoretischen Physik I (German). Spektrum, 2009.,” vol. 13, pp. 1–113, 2003, [Online]. Available: https://doi.org/10.1007/978-3-642-55432-2.

[15] P. A. M. Dirac, “A new notation for quantum mechanics,” *Math. Proc. Cambridge Philos. Soc.*, vol. 35, no. 3, pp. 416–418, 1939, DOI: 10.1017/S0305004100021162.

[16] Lang, C. & Pucker, N. *Mathematische Methoden in der Physik*. (Springer Berlin Heidelberg, 2005).

[17] Koch, W. & Holthausen, M. C. A Chemist’s Guide to Density Functional Theory. in (2000).

[18] A. Szabo and N.S. Ostlund. Modern Quantum Chemistry. McGraw-Hill, 1989.

[19] F. Schwabl. Quantenmechanik: Eine Einführung (German). Springer, 2007.

[20] W. Kohn. Nobel lecture: Electronic structure of matter-wave functions and density functionals. Reviews of Modern Physics, 71:12531266, 1999.

[21] P.O. Löwdin. Scaling problem, virial theorem, and connected relations in quantum

mechanics. Journal of Molecular Spectroscopy, 3:4666, 1959

[22] M. Odelius and I. Josefsson. Quantum chemistry - lecture notes, 2009

[23] P. Hohenberg and W. Kohn. Inhomogeneous electron gas. Physical Review, 136:B864B871, 1964

[24] L. H. Thomas Proc. Cambridge Philos. Soc., 23:542, 1927.

[25] E. Fermi. Z. Phys., 48:73, 1928.

[26] R. O. Jones and O. Gunnarsson.Rev. Mod. Phys., 61:689, 1989.

[27] G. D. Mahan.*Many-Particle Physics*.Plenum Press, New York, and London,1990.

[28] E. Teller. Rev. Mod. Phys., 34:627, 1962.

[29] N. Balázs.Phys. Rev., 156:42, 1967.

[30] E. H. Lieb and F. Y. Wu.Phys. Rev. Lett., 31:681, 1968.

[31] J. C. Phillips.*Phys. Rev.*, 112:685, 1958.

[32] W. Kohn and L. J. Sham *Phys. Rev.* **140**, A1133 (1965)

[33] R. G. Parr and W. Yang *Density Functional Theory of Atoms and Molecules* Oxford University Press, Oxford (1989)

[34] A. Szabo and N. S. Ostlund *Modern Quantum chemistry* MacMillian, New York(1982)

[35] Zenebe Assefa Tsegaye. Density functional theory studies of electronic and optical properties Of ZnS alloyed with Mn and Cr. Condensed Matter Physics, pages 11–13, 2012.

[36] Errol G. Lewars. Computational Chemistry: Introduction to the Theory and Applications of Molecular and Quantum Mechanics. Springer, 2010.

[37] A. Kabita and B. Indrajit Sharma. First-principles study on structural, phase transition, and Electronic structure of zinc sulfide ZnS within LDA, GGA, and mBJ potential. Journal of Physics, 2016.

[38] L. Mehdaouia, R. Miloua, M. Khadraoui, M.O. Bensaid, D. Abdelkader, F. Chiker, A. Bouzidi, Phys. B Condens. Matter 564 (2019) 114–124.

[39] Zhiping Yin. Microscopic mechanisms of magnetism and superconductivity studied from

First principle calculations. Pages 7, 8, 2009.

[40] Structural, electronic, and optical modeling of perovskite solar materials ASnX3 (A = Rb, K; X = Cl, Br): First principle investigations."

[41] Sachs, M., Solid State Theory, (New York, McGraw-Hill Book Company, 1963),pp159 -160;238-242

[42] Ephraim Babu, K., Murali, N., Vijay Babu, Taddesse, V.andVeeraiah,2014.

[43] S. A. Dar, V. Srivastava, U. K. Sakalle, Mater. Res. Exp. 2017, 4, 086304.

[44] S. A. Dar, V. Srivastava, U. K. Sakalle, J. Electron. Mater. 2017, 46, 6870

[45] M. Jamal, S. J. Asadabadi, I. Ahmad, H. R. Aliabad, Comput. Mater. Sci. 2014, 95, 592

[46] F. Mouhat, F. X. Coudert, Phys. Rev. B 2014, 90, 224104.

[47] M. Born, On the stability of crystal lattices. I. in Mathematical Proceedings of the Cambridge Philosophical Society, Vol. 36, No. 2, Cambridge UniversityPress, Cambridge University 1940, April, p. 160.

[48] "Y. Kong, Y. Duan, L. Ma, R. Li, Mater. Res. Exp. 2016, 3, 106505.

[49] A. Iftikhar, A. Ahmad, I. Ahmad, M. Rizwan, Int. J. Mod. Phys. B 2018, 32, 1850045.

[50] S. F. Pugh, "XCII. Relations between the elastic moduli and the plastic properties of polycrystalline pure metals," London, Edinburgh, Dublin Philos. Mag. J. Sci., vol. 45, no. 367, pp. 823–843, Aug. 1954, DOI: 10.1080/14786440808520496.